Silanes as New Highly Efficient Co-initiators for Radical Polymerization in Aerated Media

ARTICLE *in* MACROMOLECULES · FEBRUARY 2008

Impact Factor: 5.8 · DOI: 10.1021/ma702301x

Silanes as New Highly Efficient Co-initiators for Radical Polymerization in Aerated Media

J. Lalevée,* A. Dirani, M. El-Roz, X. Allonas, and J. P. Fouassier

Department of Photochemistry, UMR CNRS 7525, University of Haute Alsace, ENSCMu, 3 rue Alfred Werner, 68093 Mulhouse Cedex, France

Received October 16, 2007; Revised Manuscript Received December 23, 2007

ABSTRACT: A large series of silanes are proposed as new co-initiators for radical photopolymerization. Silanes in the presence of benzophenone, isopropylthioxanthone, camphorquinone, or dyes (Eosin) are found highly reactive and, in many cases, even better than a reference amine co-initiator (ethyl dimethylaminobenzoate (EDB)). The ability of the silanes to initiate the polymerization process under air is excellent (better than with amines), and the inhibiting effect is reduced or eliminated. An enhancement of the polymerization rates R_p under air is even sometimes noted. For example, using isopropylthioxanthone/tris(trimethylsilyl)silane, R_p increases by a 2-fold factor when going from a laminate to an aerated medium. The hardness and the hydrophobic properties of the coatings have also been evaluated. The reaction mechanisms are discussed on the basis of laser flash photolysis experiments. Specific reaction pathways explain the unusual behavior under air.

Introduction

Different varieties of radicals are now clearly recognized as powerful polymerization initiating agents. This is for example the case of the benzoyl, phosphinoyl, or aminoalkyl radicals generated from type I cleavable photoinitiators PI (benzoin ethers, bis(acylphosphine oxide)s, hydroxyalkylphenyl ketones, etc.) and type II photoinitiating systems based on a hydrogen transfer reaction between a photoinitiator PI (e.g., benzophenone, etc.) and a co-initiator coI (such as an amine).[1−4] The search for new radicals having enhanced or specific properties presents an outstanding interest.

A strong drawback for the radical polymerization reaction is the well-known inhibition by oxygen (Scheme 1): both the initiating and propagating radicals are scavenged by O_2 and yield peroxyl radicals through a peroxylation reaction. These latter species—which are not reactive toward the monomer double-bond opening—cannot initiate or participate in any polymerization reactions, thereby leading to the observed inhibition.[1−4]

As the UV-curing of acrylate resins is usually carried out in the presence of air, this has always been a key issue. Overcoming this unwanted reaction has turned into a major challenge. Up to now, different strategies have been adopted: (i) the use of laminated conditions for the photopolymerization process;[5] (ii) the use of inert atmosphere (nitrogen, argon, carbon dioxide);[6−8] (iii) the addition of amines which are assumed to readily undergo a chain peroxidation reaction leading to a strong O_2 consumption;[9] (iv) the conversion of O_2 to its excited singlet state $^1O_2$ that can be scavenged by an adequate compound (for example, an isobenzofuran derivative);[10] (v) the increase of the intrinsic reactivity of the photoinitiating system (polymerization with higher light intensity or higher photoinitiator concentration).[7−8,11] All these approaches have clearly drawbacks and limitations for practical or industrial applications.

The development of radical photoinitiating systems less sensitive to O_2 remains a fascinating problem. Up to now, silyl radicals have not received a strong interest in photopolymerization reactions. This is mainly ascribed to their unknown or supposed inefficient reactivity in the initiation step of the radical polymerization.[12] The lack of data has clearly limited the development of these systems.[13] During the course of our recent works on the experimental and theoretical studies on the reactivity of silyl radicals, we have demonstrated that (i) carefully selected species were highly efficient for the addition to monomer double bonds and (ii) the role of a particular silane (tris(trimethylsilyl)silane (TTMSS)) briefly mentioned as a co-initiator in a polymerization carried out under air was promising.[14]

Scheme 1

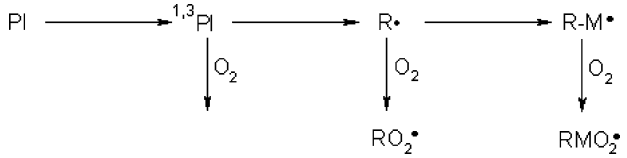

The aim of the present paper corresponds to (i) an assessment of the photoinitiation ability of a large series of new silane structures (Scheme 2) in type II photoinitiating systems based on benzophenone (BP), isopropylthioxanthone (ITX), camphorquinone (CQ), and Eosin (EO), (ii) the investigation of the silane efficiency under air, (iii) a comparison of the silanes with another largely used co-initiator (ethyl dimethylaminobenzoate (EDB)),[1] and (iv) a discussion of the corresponding reactivity based on the observation of the radicals by the laser flash photolysis LFP technique.

Experimental Section and Methodology

(i) Silanes and Photoinitiators. The silanes shown in Scheme 2—triethylsilane (**1a**), dimethylphenylsilane (**1b**), diphenylsilane (**1c**), triphenylsilane (**1d**), tris(trimethylsilyl)silane (**1e**), *N*,*N*-diethyl-1,1-dimethylsilylamine (**1f**), 1,1,3,3-tetramethyldisilazane (**1g**), *N*,*N*′,*N*″-tri-*tert*-butylsilanetriamine (**1h**), pentamethyldisilane (**1i**), 1,1,3,3,5,5 hexamethyltrisiloxane (**1j**), poly(dimethylsiloxane) hydride terminated (**1k** with M_n = 580), poly(dimethylsiloxane) hydride terminated (**1l** with M_n = 17 500), diisopropyl(3,3,4,4,5,5,6,6,6-nonafluorohexyl)silane (**1m**), *N*,*N*′-di(trimethylsilyl)methylamine (**1n**), tetrakis(dimethylamido)silane (**1o**), chlorodiphenylsilane (**1p**), 2,4,6,8 tetramethylcyclotetrasiloxane (**1q**), tris(trimethylsilyloxy)-silane (**1r**), tris(dimethylsilyloxy)phenylsilane (**1s**), 1,4-bis(dimethylsilyl)benzene (**1t**), and octadecylsilane (**1u**)—were obtained

* Corresponding author. E-mail: j.lalevee@uha.fr.

10.1021/ma702301x CCC: $40.75
Published on Web 02/19/2008

Scheme 2

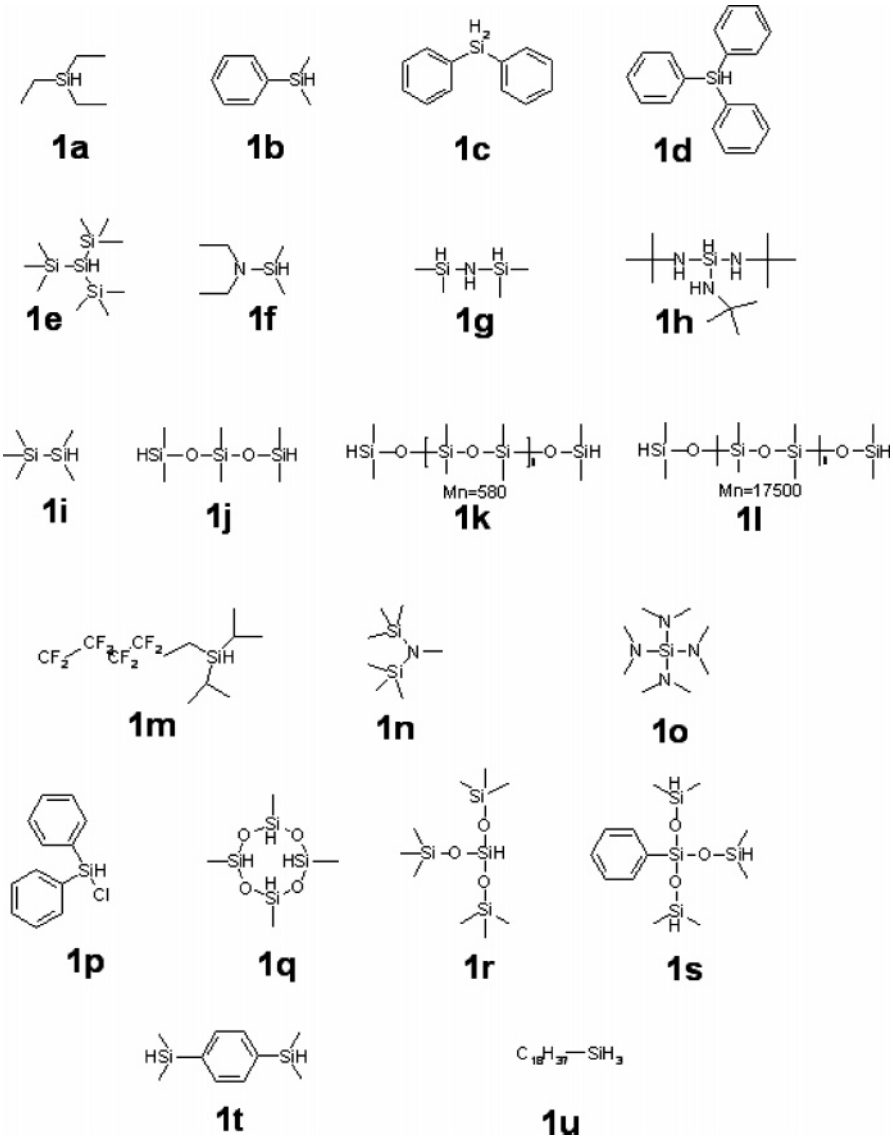

from Aldrich. *The compounds **1n** and **1o** do not correspond to co-initiators bearing Si−H bonds (silyl radicals cannot be generated). Nevertheless, these structures were added to investigate the effect of the silicon atom substituent in the amine co-initiator reactivity*. Benzophenone (BP), isopropylthioxanthone (ITX), camphorquinone (CQ), and Eosin (EO) were used as photoinitiators (Aldrich). Ethyldiethylaminobenzoate (EDB; Esacure EDB from Lamberti) was chosen as a reference amine co-initiator.

(ii) Photopolymerization Experiments. For film polymerization experiments, a given PI was dissolved into HDDA (1,6-hexanediol diacrylate from Cytec Brussels) or a bulk oligomer/monomer formulation based on 75/25 w/w epoxyacrylate/tripropylene glycol diacrylate (Ebecryl 605 from Cytec). In order to get a good reproducibility of the experiments, thin samples with low PI optical densities were used. These experimental conditions allow a good dissipation of the heat produced during the polymerization reaction and avoid any internal filter effects.[15] The laminated films (25 μm thick) deposited on a BaF_2 pellet were irradiated with the polychromatic light of a Xe−Hg lamp (Hamamatsu, L8252, 150 W). For the visible light polymerization experiments, a xenon lamp (Hamamatsu L8253, 150 W) was used (a filter was added in order to select an irradiation with $\lambda > 400$ nm). These experiments were carried out both in laminated and under air conditions.

The evolution of the double bond content was continuously followed by real time FTIR spectroscopy (Nexus 870, Nicolet).[15,16] The R_p quantities refer to the maximum rates of the polymerization reaction and were calculated from the maximum of the first derivative of the conversion vs time curves. This corresponds to the early time of the polymerization (the maximum polymerization rate is obtained from conversion between 0 and 10%). Accordingly, the monomer concentration is taken as the initial bulk concentration $[M]_0$.

(iii) Laser Flash Photolysis Experiments. Nanosecond laser flash photolysis (LFP) experiments were carried out using a Q-switched nanosecond Nd/YAG laser ($\lambda_{exc} = 355$ nm, 9 ns hwhm pulses; energy reduced down to 10 mJ, from Powerlite 9010 Continuum) and an analyzing system consisting of a pulsed xenon lamp, a monochromator, a fast photomultiplier, and a transient digitizer.[17]

The hydrogen abstraction rate constants wit *t*-BuO$^\bullet$ were determined by a classical Stern−Volmer treatment using the rising time of the Si$^\bullet$ (or C$^\bullet$ in the case of **1n** and **1o**) species for the different silane concentrations. The interaction rate constants ^{3}BP (or ^{3}ITX)/silane are determined by a Stern−Volmer treatment from the triplet state lifetimes observed at 525 nm (or 600 nm). The ketyl radical quantum yield ($\Phi_{K\bullet}$) in the case of benzophenone was determined by a classical procedure using the absorption coefficients of both the triplet state and the ketyl radical.[17−19] For ITX, $\Phi_{K\bullet}$ was determined with respect to the system ITX/triethylamine ($\Phi_{K\bullet} = 1$) since the absorption coefficient for the ketyl radical is unknown. For this compound, the ketyl radical was readily observed at 480 nm.

(iv) ESR Spin Trapping Experiments. ESR spin trapping experiments were carried out on a X-band spectrometer (MS 200 Magnettech). This technique is now recognized as particularly powerful for an identification of the radical center (Si, N, or C in the present case). The radicals generated in ^{3}BP/coI are trapped by phenyl-*N*-*tert*-butylnitrone (PBN).

(v) Final Polymer Properties. The hardness of the cured film was evaluated on 100 μm thick UV cured films coated onto a glass plate by monitoring the damping of the oscillations of a pendulum (Persoz hardness, elcometer 3030), which is directly related to the softness of the sample.

Contact angle measurements θ (water/polymer) were also carried out for a characterization of the hydrophobic character of the polymer surface (Digidrop-GBX Scientific Instruments). As previously, 100 μm thick UV-cured films coated onto a glass plate were used, and the contact angle value corresponds to an average of three experiments (the change of θ was lower than 3% for all the experiments).

Results and Discussion

1. Silanes as Efficient Co-initiators under UV or Visible Light Irradiations. Assuming that the termination of the polymerization occurs through a bimolecular process, the rate of polymerization R_p is expressed by eq 1 (this is usually considered as true in film photopolymerization experiments[1−4]) where k_p is the propagation rate constant, k_t the termination rate constant, and R_i the initiation rate as defined in eq 2. In this expression, I_{abs} is the amount of light absorbed and ϕ_i represents the initiation quantum yield that corresponds to the number of starting polymer chains per photon absorbed. The relative initiation efficiency ϕ_{rel} of a given photoinitiating system PI is expressed with respect to that of a reference PIr (eq 3).

$$R_p = k_p\left(\frac{R_i}{K_t}\right)^{1/2}[M] \quad (1)$$

$$R_i = \phi_i I_{abs} \quad (2)$$

$$\phi_{rel} = \frac{\phi_i(Pl)}{\phi_i(Plr)} \quad (3)$$

Taking into account that all rates of polymerization should be corrected for the amount of energy absorbed by each sample, ϕ_{rel} is calculated from the conversion curves according to eq 4, where R_p(PI) and R_p(PIr) are the rates of polymerization in the presence of the photoinitiator (PI) and the reference photoinitiator (PIr), respectively. I_{abs}(PI) and I_{abs}(PIr) are the amounts of energy absorbed by PI and PIr. EDB is used as a reference. In our experimental conditions, only the photoinitiator absorbs the light delivered by the lamp: an identical I_{abs} value is considered for both the PI/EDB and PI/silane systems. Therefore, the square of the R_p ratio gives a direct access to ϕ_{rel}. Under this approach, a direct comparison of the initiation abilities of the silanes with the reference amine can be obtained.

$$\phi_{rel} = \left(\frac{R_p(Pl)}{R_p(Plr)}\right)^2 \frac{I_{abs}(Plr)}{I_{abs}(Pl)} \quad (4)$$

The polymerization rates of a viscous monomer (Ebecryl 605) as well as the relative initiation quantum yields Φ_{rel} for the different PI/silane combinations are gathered in Tables 1−4. The polymerization rates are given both in laminated and under air conditions: the R_p changes expressed in percentage are also indicated to outline the oxygen effect on the radical polymerization reaction.

Table 1. Polymerization Rates of Ebecryl 605 Using a Benzophenone/Silane Type II Photoinitiating System (1%/1%, w/w) Irradiated under the Xenon−Hg Lamp

	laminated conditions	under air		
co-initiator	$R_p/[M_0] \times 100$[a]	$R_p/[M_0] \times 100$[b]	hardness (s)[c]	contact angle (θ), deg
EDB	25.6	21 (−18%)	300	56
1a	36 (1.97)	32 (−11%)		
1b	22.7 (0.78)	23.9 (+5%)		
1c	33.6 (1.72)	32.1 (−4.5%)	312	53
1d	22 (0.74)	18.2 (−17%)		
1e	30.5 (1.41)	35.1 (+15%)	320	
1f	31 (1.46)	28.1 (−9%)	337	
1g	42 (2.7)	27.1 (−35%)	340	
1h	40.7 (2.52)	28.5 (−29%)		
1i	33 (1.66)	34.3 (+4%)		
1j	42.1 (2.7)	32.1 (−23%)	316	52
1k	39.2 (2.34)	33.8 (−13%)		
1l	33.8 (1.74)	37.2 (+10%)	323	78
1m	32.4 (1.6)	32.8 (+1%)	313	52
1n	46.0 (3.22)	35.2 (−23%)	323	59
1o	45.9 (3.21)	39.1 (−15%)	315	55
1p	42.3 (2.75)	38.1 (−10%)	311	51
1q	47.1 (3.38)	31.7 (−32%)	275	91
1r	34.1 (1.77)	27.4 (−19%)	285	56
1s	42.4 (2.74)	33.7 (−20%)	305	59
1t	36.6 (2.04)	34.9 (−5%)	335	56
1u	35.7 (1.95)	26.9 (−24%)	295	84

[a] ϕ_{rel} are given in parentheses. [b] The R_p decrease or increase from laminated to aerated conditions are given in parentheses. [c] Persoz hardness of the tack-free film.

Table 2. Polymerization Rates of Ebecryl 605 Using an Isopropylthioxanthone/Silane Type II Photoinitiating System (1%/1%, w/w) Irradiated under the Xenon−Hg Lamp

	laminated conditions	under air		
co-initiator	$R_p/[M_0] \times 100$[a]	$R_p/[M_0] \times 100$[b]	hardness (s)[c]	contact angle (θ), deg
EDB	37.5	29.2 (−22%)	320	54
1a	16.4 (0.17)	21.7 (32%)		
1b	18.1 (0.24)	19.6 (8%)		
1c	12.6 (0.11)	16.4 (30%)	356	56
1d	19.9 (0.28)	15.2 (−23%)	306	
1e	13.4 (0.13)	28.3 (113%)	343	56
1f	30.8 (0.67)	37.8 (22%)	340	69
1g	38.7 (1.06)	33.5 (−13%)	340	60
1h	31.5 (0.71)	25.0 (−20%)	285	
1i	15.8 (0.18)	21.3 (34%)		
1j	13.3 (0.12)	14.4 (10%)	350	53
1k	18.6 (0.24)	17.3 (−6%)	*d*	91
1l	21.5 (0.33)	22.1 (3%)	*d*	88
1m	19.7 (0.28)	16.2 (−17%)	349	
1n	56.6 (2.27)	34.5 (−39%)	358	
1o	59.7 (2.53)	35.7 (−40%)	347	
1p	12.0 (0.1)	13.5 (12%)	340	60
1q	27 (0.52)	22.1 (−18%)	*d*	101
1r	22.3 (0.35)	15.2 (−31%)	357	59
1s	21 (0.31)	22.7 (8%)	358	58
1t	17.7 (0.22)	14.5 (−18%)	335	57
1u	7.8 (0.04)	6.1 (−21%)	263	89

[a] ϕ_{rel} are given in parentheses. [b] The R_p decrease or increase from laminated to aerated conditions are given in parentheses. [c] Persoz hardness of the tack-free film. [d] Slippery surface: the Persoz hardness cannot be determined.

The reported results cannot be directly compared from one table to another as the experimental conditions—particularly the light source (Xe lamp vs Xe−Hg lamp) and the light intensity—are changed. However, the EDB efficiency in the presence of BP, ITX, and CQ can be evaluated taking into account the energy absorbed so that normalized data become accessible. Under the present irradiation conditions, the relative amounts

Table 3. Polymerization Rates of Ebecryl 605 Using a Camphorquinone/Silane Type II Photoinitiating System (1%/1%, w/w) Irradiated under the Xenon Lamp

	laminated conditions	under air	
co-initiator	$R_p/[M_0] \times 100^a$	$R_p/[M_0] \times 100^b$	hardness (s)^c
EDB	19.9	17.9 (−10%)	290
1b	14.8 (0.53)	17.7 (+19%)	
1d	14.8 (0.53)	13.7 (−7%)	
1e	35.8 (3.23)	33.5 (−6%)	320
1f	25.1 (1.59)	20.5 (−18%)	338
1g	16.3 (0.67)	15.5 (−5%)	
1h	28.8 (2.09)	16.8 (−41%)	
1j	15.5 (0.61)	13.4 (−13%)	
1k	15.0 (0.57)	13.3 (−11%)	347

[a] ϕ_{rel} are given in parentheses. [b] The R_p decrease or increase from laminated to aerated conditions are given in parentheses. [c] Persoz hardness of the tack-free film.

Table 4. Polymerization Rates of Ebecryl 605 Using an Eosin/silane Type II Photoinitiating System (0.1%/1%, w/w) Irradiated under the Xenon Lamp in Aerated Conditions

co-initiator	$R_p/[M_0] \times 100$	co-initiator	$R_p/[M_0] \times 100$
EDB	0.47	**1g**	0.24
1c	0.24	**1j**	0.9
1f	1.0	**1t**	0.36

of absorbed energy I_{abs} are 1, 2.5, and 0.05 for BP, ITX, and CQ, respectively. The relative R_p obtained in the presence of the different PI can be calculated using eqs 1 and 2.

The two significant points are (i) the general high reactivity of the silanes compared to EDB (the different PI/silanes can clearly be considered as new efficient co-initiators) and (ii) the high efficiency under air. These results will be now discussed for the different PIs.

(i) BP/Silanes. When using BP (Table 1) in laminated and under air conditions, only **1b** and **1d** are characterized by an efficiency lower than with EDB (Table 1, Figure 1). The best values are obtained with **1g**, **1h**, **1j**, **1k**, **1p**, **1q**, and **1s** where the R_p increase is higher than 60% compared to EDB. Silylamines (**1n**, **1o**) also exhibit an enhanced reactivity demonstrating the interest of the presence of a silicon atom onto the amines; however, in aerated conditions, a strong inhibition is noted with a drop of R_p about 40%.

Interestingly, silanes are not found so drastically affected by O_2. For EDB, the R_p decreases by about 20% under air compared to laminated conditions. Compounds **1b**, **1c**, **1e**, **1i**, **1k**, **1l**, **1m**, **1p**, and **1t** exhibit an oxygen sensitivity lower than the reference amine. In some cases (**1b**, **1e**, **1i**, and **1l**), an enhanced reactivity is even observed. Some silanes are not really inhibited. For the others, a decrease of the polymerization rates is observed under oxygen albeit this inhibition remains modest; i.e., only **1d** is found noticeably less efficient than the reference amine under air.

(ii) ITX/Silanes. A less interesting relative behavior of the silanes with respect to EDB is noted when BP is changed for ITX (Table 2). In laminated or under air conditions, only **1g**, **1n**, **1o** and **1f**, **1g**, **1n**, **1o** are better than EDB (Table 2). From a general point of view, the compounds that are efficient with BP are also found efficient with ITX. When using EDB under air, the same decrease of R_p (about 20% as for BP) is observed (Table 2). Silanes exhibiting a weak oxygen inhibition in the presence of BP are also very efficient with ITX (**1b**, **1c**, **1e**, **1i**, **1k**, **1l**, **1m**, **1p**). Some other ones (**1a**, **1f**, **1j**, **1s**) appear as more efficient under O_2 when using ITX. For **1a**, **1c**, **1e**, **1f**, **1i**, and **1p**, a significant positive effect of oxygen is noted.

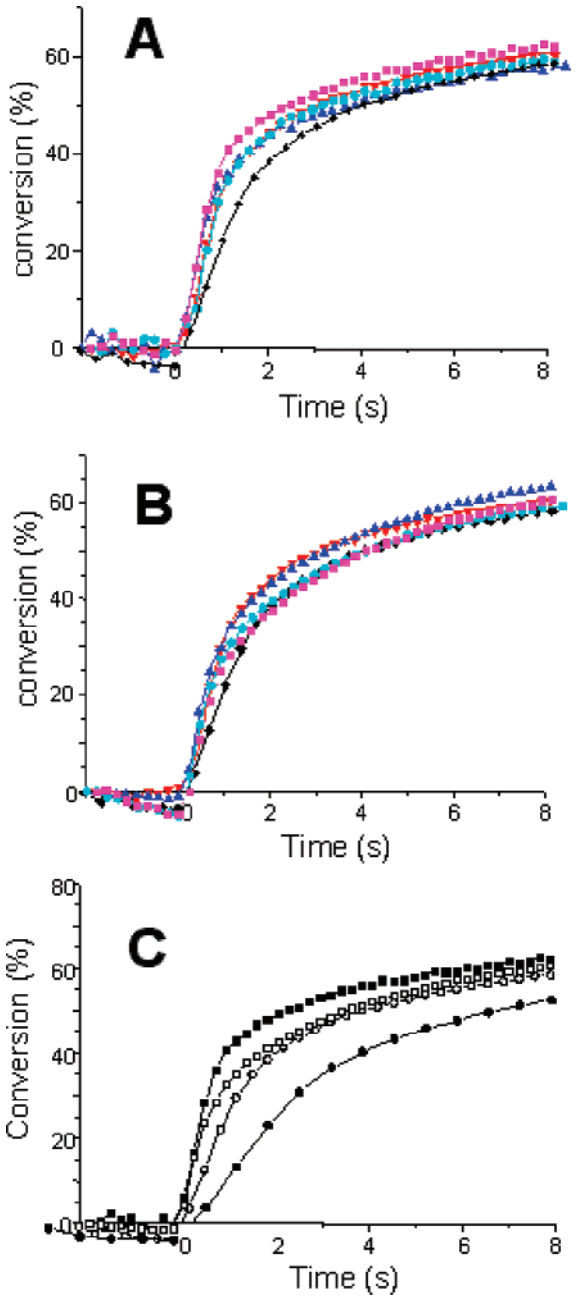

Figure 1. Conversion vs time curves for the photopolymerization of Ebecryl 605. photoinitiating system: BP/co-initiator 1%/1% w/w EDB (diamond); **1c** (square); **1s** (down triangle); **1t** (up triangle); **1u** (circle): (A) laminated conditions and (B) under air. (C) Photoinitiating system: ITX/co-initiator 1%/1% w/w EDB (square) and **1e** (circle): laminated conditions (full symbol); under air (open symbol).

(iii) Visible Light Systems: CQ/Silanes and EO/Silanes. The efficiency of some selected silanes has been checked to demonstrate the interest of the new proposed co-initiators for polymerization under visible light using a ketone (CQ) or a dye (EO) as a photoinitiator (Tables 3 and 4). For CQ, the silanes **1e**, **1f**, and **1h** are more efficient than EDB in both laminated or aerated conditions. For EO, compounds **1f** and **1j** are found 2 times more reactive than EDB under air. These results show that silanes are also interesting for visible light induced polymerization in aerated conditions.

(iv) Final Polymer Properties. From a qualitative point of view, the silanes used here lead to tack free coatings under O_2. For a more refined analysis, the hardness and the contact angles (water/polymer) were used to characterize the final polymer

Table 5. Polymerization Rates of HDDA Using Isopropylthioxanthone/Silane (1%/1%, w/w) Photoinitiating System Irradiated under the Xenon−Hg Lamp in Laminates

co-initiator	$R_p/[M_0] \times 100^a$	relative R_p in HDDA	relative R_p in Ebecryl 605
EDB	12.2	1	1
1b	5.1	0.41	0.48
1d	5.6	0.46	0.53
1e	5.8	0.48	0.35
1f	14.6	1.2	0.82
1g	6.5	0.53	1.03
1h	10.1	0.83	0.84
1i	5.4	0.44	0.42
1k	6.2	0.50	0.50

[a] The light intensity is 4 times lower than in the experiments carried out in Table 2.

properties of the coating formed in aerated conditions. Results are shown in Tables 1−4.

With silanes, higher surface hardnesses than those obtained with EDB are measured (with an average increase of 5−15%). The highest values obtained for ITX/**1c**, ITX/**1r**, and ITX/**1s** (356, 357, and 358 s) are promising for an improvement of the surface properties for practical applications.

Regarding the contact angles, the silanes do not drastically change the surface character properties (typical values between 52° and 60°). For EDB, a value of 54°−56° is usually obtained. However, interestingly, the siloxane derivatives (**1k**, **1l**, **1q**) lead to a strong hydrophobic character (values between 85° and 101°). This can be ascribed to the polydimethylsiloxane PDMS units (already known for their hydrophobic properties[20]) incorporated in the polymer surface. Compound **1j** does not lead to high values thereby demonstrating the role of the siloxane chain length. *The behavior of the siloxane compounds used in the photoinitiating system is highly interesting for practical applications requiring high hydrophobic surfaces.*

(v) Viscosity Effect. In order to check the effect of the formulation viscosity, the photopolymerization of HDDA in the presence of selected ITX/silane couples was carried out in laminate (Table 5). The efficiency order of the different silanes is almost the same in HDDA and Ebecryl 605, except for **1f** and **1g**.

2. (Photo)chemical Mechanisms Associated with the Silanes Reactivity. Some LFP experiments were carried out for a better understanding of the properties of these new co-initiators (Figure 2). The experiments were restricted to carefully selected samples exhibiting either a good or a bad performance in photopolymerization. A complete study of silyl radicals reactivity is beyond the scope of the present paper. More detailed and highly useful investigations are given in ref 13.

(i) Hydrogen Abstraction Reaction. The silyl radicals were generated from an hydrogen transfer reaction between *tert*-butoxyl radical and the silane. The solvent used is di-*tert*-butylperoxide/benzene (50%/50%). Basically, the reaction consists of two consecutive steps as already proposed.[21−23] The first step is the generation of a *tert*-butoxyl radical through the photochemical decomposition of di-*tert*-butyl peroxide; the second step corresponds to a Si−H hydrogen abstraction reaction from the silane (except for **1n**, **1o** where a α C−H abstraction occurs), respectively, which generate the expected radical. The hydrogen abstraction rate constants with *t*-BuO$^\bullet$ were determined by a classical Stern−Volmer treatment using the rising time of the Si$^\bullet$ (or C$^\bullet$ in the case of **1n**, **1o**) species for the different silane concentrations. The silyl radical adds to a double bond and forms a radical adduct (Scheme 3) that can be observed as presented in ref 14, allowing a direct access to the addition rate

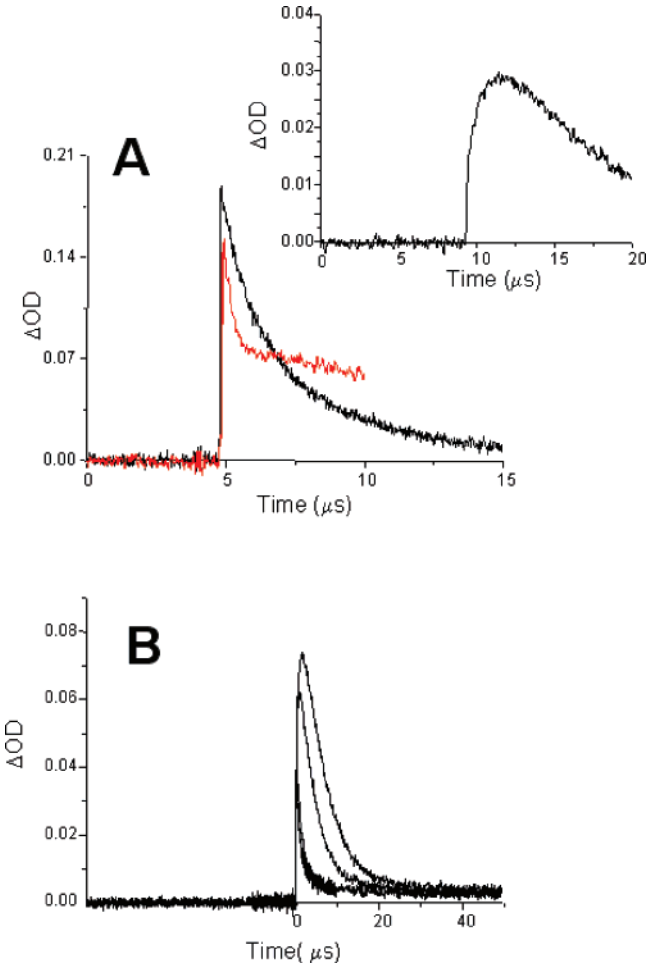

Figure 2. (A) Interaction of ^{3}BP with **1d**; kinetic trace at 525 nm for [**1d**] = 0 and 0.08 M, respectively. Inset: silyl radical formation for [**1d**] = 0.025 M at 330 nm obtained in the *t*-BuO$^\bullet$/**1d** system in di-*tert*-butyl peroxide. (B) Determination of k_{add} for **1d**: decay of the silyl radical at 330 nm for different methyl acrylate concentrations [MA] (0, 0.0004, 0.002, and 0.0028 M).

Scheme 3

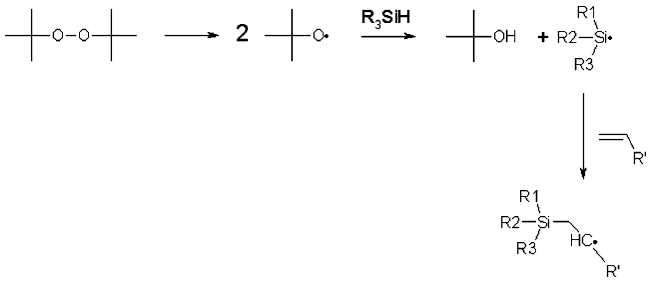

constants k_{add}. For **1d**, the silyl radical strongly absorbs in the UV range; k_{add} is therefore determined from the decay time of this species.

A second way for the silyl radicals formation consists in the interaction between the ketone (BP or ITX) triplet state and the silane (solvent: benzene). The interaction rate constants were determined through the observation of the triplet state at 525 and 600 nm for BP and ITX, respectively.[17]

The hydrogen abstraction rate constants between the *tert*-butoxyl radical or the ketone triplet states (^{3}BP or ^{3}ITX) and the silanes are high (Table 6): they range from 3×10^6 to 8.5×10^7 M^{-1} s^{-1}, 4.3×10^6 to 3.1×10^7 M^{-1} s^{-1}, and 10^5 to 4.1×10^7 M^{-1} s^{-1} for *t*-BuO$^\bullet$, ^{3}BP, and ^{3}ITX, respectively (Table 6, Figure 2). The high rate constants observed with *t*-BuO$^\bullet$

Table 6. Rate Constants and Quantum Yields Characterizing the Formation and the Reactivity of the Silyl Radicals (See Text)

	BP[a]		ITX[a]		*t*-Bu−O•	MA
	k_q, $M^{-1} s^{-1}$	Φ_K•	k_q, $M^{-1} s^{-1}$	Φ_K•	k_H, $M^{-1} s^{-1}$	k_{add}, $M^{-1} s^{-1}$
1a	4.3×10^6 (9.6×10^6 [d])	0.81	7.2×10^5	0.3	1.0×10^7 (5.7×10^6 [d])	2.4×10^8
1b	2.5×10^7 (8.8×10^6 [d])	0.65	3.4×10^7	0.28	1.5×10^7 (6.6×10^6 [d])	4.510^8 (3.65×10^8 [c])
1d	3.1×10^7	0.75	7.7×10^6	0.21	6.7×10^7 (1.1×10^7 [d])	5.1×10^8
1e	1.02×10^8 (3.4×10^8 [d])	0.95	4.1×10^7	0.7	8.5×10^7 (1.1×10^8 [d])	2.2×10^7
1f	1.1×10^9	0.9	1.5×10^8	0.3 (0.7[b])	2.5×10^8	3.3×10^7
1g	2.2×10^7	0.78	1.6×10^6	0.34	2.5×10^7	1.5×10^8
1h	6.1×10^8	0.24	9.1×10^7	0.1 (0.26[b])	2.2×10^7	7.9×10^7
1j	2.1×10^7	0.66[b]	10^5	0.2	$3.0\ 10^6$	$2.0\ 10^8$
1q	5.0×10^6	0.45[b]	nd[e]	nd	$1.5\ 10^7$	$5.1\ 10^7$

[a] In benzene. [b] In acetonitrile. [c] For methyl methacrylate (MMA). [d] References 13a−13d. [e] nd = not determined.

outline the labile hydrogen character of the silanes. The values are lower than those usually found with amines (in the 10^8 M^{-1} s^{-1} range).[24] Much higher hydrogen abstraction rate constants were also measured for the BP (or ITX) triplet state/amine interaction which corresponds to an electron/proton-transfer reaction.[17] For the silanes, the oxidation potential are higher than 2 V for **1a**−**1d**; a lower value of 1.7 V was determined for **1e** (present work). Using a reduction potential of −1.79 V and a triplet state energy of 2.98 eV for BP, an endothermic electron-transfer reaction (higher than +0.41 eV) can be expected from the classical Rehm−Weller equation eq 5,[25] where ΔG_{et}, E_{ox}, E_{red}, E_T, and C are the free energy change for the electron-transfer reaction, the oxidation potential of the donor, the reduction potential of the acceptor, the triplet state energy, and the Coulombic term for the formed initial ion pair, respectively. This result supports the fact that the ^{3}BP (and ^{3}ITX)/ silane reaction probably corresponds to a pure hydrogen transfer process and not to an electron/proton-transfer sequence.

$$\Delta G_{et} = E_{ox} - E_{red} - E_T + C \quad (5)$$

For the silylamines [**1f**, **1g**, **1h**], an electron/proton-transfer sequence probably occurs; i.e., high rates with ^{3}BP (and ^{3}ITX) are obtained. This is in agreement with the low oxidation potential of these compounds (for example for **1f**, E_{ox} = 1.1 V), leading to an exothermic electron-transfer process.

The quantum yields in ketyl radicals in the BP/silane combinations (which are obviously equal to the quantum yields in silyl radicals Φ_{Si}) are very high (close to 1 for **1e**). Interestingly, lower Φ_{Si} are observed in ITX/silane. This is in agreement with the intrinsic lower initiation quantum yields observed in the ITX/silane formulations. In acetonitrile, a solvent which increases the nπ* character of ^{3}ITX, the Φ_{Si} values are about 3 times higher than in benzene (Table 6): this result probably evidence the sensitivity of the silanes in the hydrogen abstraction reaction toward the spectroscopic character of the lowest lying triplet state.

For **1f**, **1g**, and **1h**, two different sites for the hydrogen abstraction can be expected (α(C−H); N−H, or Si−H). From ESR spin-trapping experiments, it has been observed that these structures (when benzophenone is used as PI) lead at least to silyl radicals (Figure 3) with abstraction ratios of 35% SiH/ 65% CH for **1f**, 60% SiH/40% NH for **1g**, and >95% SiH for **1h**. For the amines (**1n**, **1o**), a α(C−H) hydrogen abstraction occurs and higher rate constants are thus observed.

(ii) Reactivity of the Silyl Radicals toward Monomers. The addition rate constants k_{add} to methyl acrylate MA determined as in Figure 2 are gathered in Table 6. A very high reactivity with rate constants ranging from 2.2×10^7 to 4.5×10^8 M^{-1} s^{-1} is noted. These k_{add} are the highest values reported up to now for well-known initiating structures such as the benzoyl (~10^5 M^{-1} s^{-1}), the aliphatic aminoalkyl (~2×10^7 M^{-1} s^{-1}), the hydroxy isopropyl (~10^7 M^{-1} s^{-1}), or the phosphinoyl radicals (~2×10^7 M^{-1} s^{-1}).[13,24] For the EDB derived radical a value of 5×10^5 M^{-1} s^{-1} was recently measured.[24] All these results demonstrate the high potential of the silyl radicals to act as photoinitiating species.

(iii) Initiation Mechanism in Laminate. A plausible initiation mechanism is displayed in Scheme 4, where S_0, S_1, and T_1 represent the singlet ground state and the excited singlet and triplet states of the photoinitiator, respectively; Rad• stands for the ketyl type radical.

The initiation quantum yield ϕ_i is connected with the yield of the hydrogen transfer reaction ϕ_H, the production yield of the free silyl radical ϕ_K and the addition yield to the monomer ϕ_{AD}:

$$\phi_i = \phi_H \phi_K \phi_{AD} \quad (6)$$

In Ebecryl 605, the rate constants are diffusion limited to a value of 4.2×10^5 M^{-1} s^{-1}: one can expect that ϕ_H is almost constant in our experimental conditions.[15] The ϕ_K values determined in solution cannot be safely extrapolated to the values in bulk (due to the in-cage processes). The addition rate constants should also leveled off to the diffusion limit. The viscosity corrected addition rate constants are the same for all silyl radicals since $k_{add} > k_{diffusion}$. Nothing can be said about ϕ_{AD}, which must be dependent on the secondary reactions of the silyl radicals as the efficiency of these reactions is a function of the considered silane. The ϕ_{AD} values cannot obviously be calculated. As a consequence, structure/reactivity relationships for the Ebecryl 605 polymerization can hardly be proposed.

On the other hand, in the HDDA matrix, the diffusion rate constant is limited to a value of 6.0×10^8 M^{-1} s^{-1}, and the rate constants determined in solution can be used.[15] For the investigated silyl radical, the addition reaction is now not limited by the diffusion as $k_{add} < k_{diffusion}$. In a first approach, the higher reactivity of the silyl radicals compared to that of EDB (k_{add} = 5×10^5 M^{-1} s^{-1}) must lead to a drastic increase of Φ_{rel}. However, interestingly, it can clearly be noted in Table 5 that the relative efficiency (compared to EDB) is almost the same in HDDA and Ebecryl 605. Moreover, the efficiency order of the different silanes is also similar in HDDA and Ebecryl 605 (a slight deviation is noted for **1g**). This result demonstrates that the initiation mechanism is not governed only by the primary processes presented in Scheme 4. The side reactions

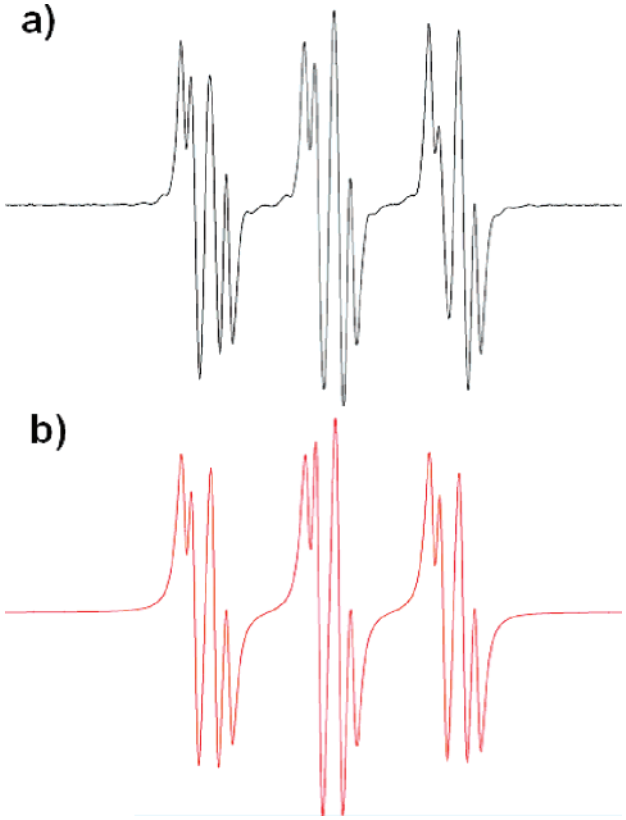

Figure 3. (a) ESR spectrum of the radicals generated in ^{3}BP/**1f** and trapped by phenyl-*N*-*tert*-butylnitrone (PBN). (b) Simulated ESR spectrum with 35% of silyl radicals [a_N = 14.8 G; a_H = 5.4 G] and 65% of aminoalkyl radicals [a_N = 14.6 G; a_H = 2.35 G].

Scheme 4

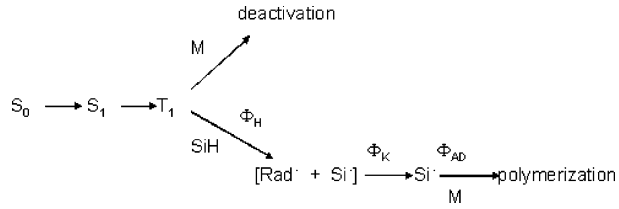

associated with the silyl radical level off the overall reactivity when going from viscous to fluid media. These side reactions will also be very important for polymerization under air.

(iv) Influence of O_2. Silanes are characterized by an excellent reactivity in aerated conditions presumably connected with the very high efficiency of the peroxylation process (I). Rate constants close to (3−4) × 10^9 M^{-1} s^{-1} are observed for this reaction (ref 13 and this work). Therefore, the silyl radicals are efficient to consume oxygen.

$$R_3Si^{\bullet} + O_2 \rightarrow R_3Si{-}O_2^{\bullet} \qquad (I)$$

Reaction II should also probably occur regenerating another silyl radical:

$$R_3Si{-}O_2^{\bullet} + R_3Si{-}H \rightarrow R_3Si{-}O_2H + R_3Si^{\bullet} \qquad (II)$$

Another interest of the silane derived peroxyl radical is the possibility of a rearrangement reaction (III) recreating a silyl radical.[26,27]

(III)

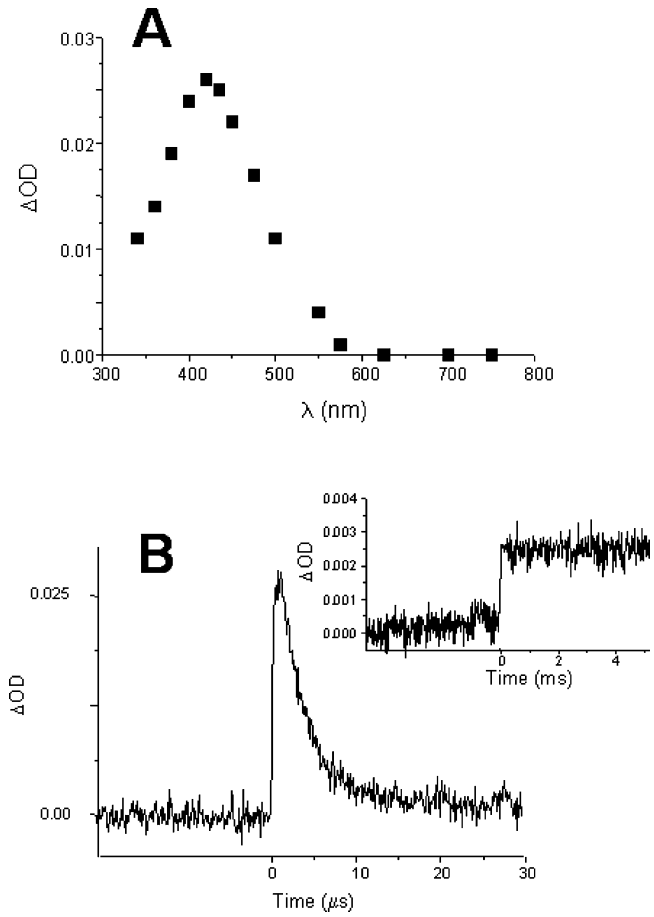

Figure 4. (A) Spectrum of the peroxyl radical of **1e** in di-*tert*-butyl peroxide in an oxygenated saturated solution. (B) Peroxyl radical decay at 400 nm (lifetime 2.5 μs). Inset: decay trace for EDB−O−O$^{\bullet}$ at 420 nm (lifetime ≫ 4 ms).

This rearrangement, previously suspected for **1e**,[27] has been directly observed in the present work by LFP. The peroxyl radical spectrum of **1e** centered around 420 nm is depicted in Figure 4. This assignment is based on the rising time which corresponds to an interaction rate constant $R_3Si^{\bullet}/O_2$ of 3.1 × 10^9 M^{-1} s^{-1}. DFT calculations predict an absorption wavelength for this peroxyl radical at about 385 nm at the TD-MPW1PW91/6-31G* level in agreement with the experimental data. The rather short lifetime for $R_3Si{-}O{-}O^{\bullet}$ (2.5 μs) can be compared to the values reported for usual peroxyl species (in the millisecond range for EDB−O−O$^{\bullet}$ in Figure 4), supporting the very efficient reorganization process ($k \sim 4 \times 10^5$ s^{-1} for **1e**). The weak absorption observed around 300 nm is ascribed to the newly formed oxygenated silyl radical. The addition of such an oxygenated silyl radical to an acrylate double bond remains very efficient as exemplified by the addition rate constant of the triethoxysilyl radical to methyl acrylate measured here (5.5 × 10^8 M^{-1} s^{-1}). Different other rearrangement mechanisms were proposed recently.[29] Particularly, the formation of a silyloxyl intermediate ($R'_3SiO^{\bullet}$) was suggested. From the final product analysis, the formation of silyl radicals is always envisaged.

For comparison, reaction III is considerably slowed for the EDB peroxyl radical as shown in Figure 3. In the same way, the reaction II for the EDB peroxyl radical/amine interaction is probably rather weak (an upper value for the EDB−$O_2^{\bullet}$/amine interaction rate constant of 200 M^{-1} s^{-1} has been determined by the method presented in detail in ref 28). Last, reaction IV efficiently contributes to the destruction of the peroxides formed

Scheme 5

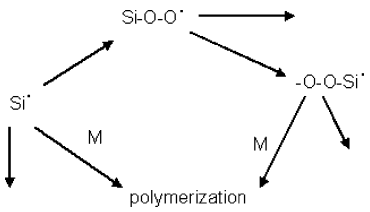

on the growing polymer chains and the generation of a very efficient initiating radical:

$$RM-O_2^{\bullet} + R_3Si-H \rightarrow RM-O_2H + R_3Si^{\bullet} \qquad (IV)$$

Finally, under polychromatic irradiation, the photodecomposition of the peroxides or hydroperoxides formed (particularly step II) can be expected (V). The generating radicals can easily abstract hydrogen atom from silanes (Table 6).

$$R_3Si-O-O-R' \rightarrow R_3Si-O^{\bullet} + {}^{\bullet}O-R' \quad (h\nu) \qquad (V)$$

The interest of the overall processes I−V is the primary oxygen consumption (I), the generation of a silyl radical (II, IV, and V), and the re-formation of a highly efficient oxygenated silyl radical (III). Both silyls can in turn initiate the polymerization. Reaction I competes with the initiating silyl radical/monomer reaction. According to the rate constants of the different primary routes shown in Scheme 5, which can be affected by the silane structures, many situations (either beneficial or detrimental) concerning the oxygen effect can be expected. These processes likely account for the oxygen low sensitivity effect observed here. The enhancement of R_p under air for different PI/silane initiating systems is mainly ascribed to reaction V. Indeed, the number of radicals produced from silanes both in air and laminate remains the same from reactions II−IV. Photopolymerization experiments using both UV and visible light irradiations for CQ are characterized by higher R_p than irradiation with $\lambda > 400$ nm. These results evidence the interest of reaction V for polymerization processes in aerated conditions. A detailed investigation of the photodecomposition of these peroxides is beyond the scope of the present paper and will be investigated in forthcoming works.

Conclusion

The silanes proposed in this study are new highly efficient co-initiators. For UV and visible lights irradiations, a lot of silanes work better than the reference amine. The remarkable behavior of the silyl radicals as photoinitiating species was clearly underlined, and some insights into their reactivity under oxygen were proposed. A new promising chemistry involving Si atom bearing photoinitiating systems likely opens up for the design of specific coating properties (polymerization rates, surface hardness, hydrophobicity, etc.). By the way, we will show the high reactivity of the silyl radicals formed from cleavable disilanes and the absence of oxygen inhibition using silanes in free radical cationic photopolymerization reactions.

References and Notes

(1) (a) Fouassier, J. P. *Photoinitiation, Photopolymerization and Photocuring: Fundamental and Applications*; Hanser Publishers: New York, 1995. (b) *Photochemistry and UV Curing: New Trends*; Fouassier, J. P., Ed.; Research Signpost: Trivandrum, 2006.

(2) Fouassier, J. P. In *Radiation Curing in Polymer Science and Technology*; Fouassier, J. P., Rabek, J. F., Eds.; Elsevier Science Publishers Ltd.: London, 1993.

(3) Dietliker, K. *A Compilation of Photoinitiators Commercially Available for UV Today*; Sita Technology Ltd.: Edinburgh, London, 2002.

(4) Rabek, J. F. *Mechanisms of Photophysical Processes and Photochemical Reactions in Polymers. Theory and Applications;* Wiley-Interscience: Chichester, 1987.

(5) Bolon, D. A.; Webb, K. K. J. *Appl. Polym. Sci.* **1978**, *9*, 2543.

(6) Wight, F. R. *J. Polym. Sci., Polym. Lett. Ed.* **1978**, *16*, 121.

(7) Studer, K.; Decker, C.; Beck, E.; Schwalm, R. *Prog. Org. Coat.* **2003**, *48*, 101.

(8) *Radiation Curing of Polymeric Materials*; ACS Symposium Ser. 417; Hoyle, C. E., Kinstle, J. F., Eds.; American Chemical Society: Washington, DC, 1989.

(9) (a) Davidson, R. S. In *Radiation Curing in Polymer Science and Technology*; Fouassier, J. P., Rabek, J. F., Eds.; Elsevier Science Publishers Ltd.: London, 1993; Vol. III. (b) Hoyle, C. E.; Kim, K. J. *J. Appl. Polym. Sci.* **2003**, *33*, 2985. (c) Decker, C.; Jenkins, A. D. *Macromolecules* **1985**, *18*, 1241.

(10) (a) Gou, L.; Opheim, B.; Scranton, A. B. In *Photochemistry and UV Curing: New Trends*; Fouassier, J. P., Ed.; Research Signpost: Trivandrum, 2006. (b) Decker, C. *Makromol. Chem.* **1979**, *180*, 2027.

(11) Awokola, M.; Lenhard, W.; Loffler, H.; Flosbach, C.; Frese, P. *Prog. Org. Coat.* **2002**, *44*, 211.

(12) (a) Arsu, N.; Hizai, G.; Yagci, Y. *Macromol. Rep.* **1995**, 1257. (b) Yagci, Y.; Reetz, I. *Prog. Polym. Sci.* **1998**, *23*, 1485.

(13) (a) Chatgilialoglu, C. *Organosilanes in Radical Chemistry*; Wiley: Chichester, 2004. (b) Chatgilialoglu, C.; Ingold, K. U.; Lusztyk, J.; Nazran, A. S.; Scaiano, J. C. *Organometallics* **1983**, *2*, 1332. (c) Chatgilialoglu, C.; Scaiano, J. C.; Ingold, K. U. *Organometallics* **1982**, *1*, 466. (d) Chatgilialoglu, C. *Chem. Rev.* **1995**, *95*, 1229. (e) Chatgilialoglu, C.; Timokhin, V. I.; Zaborovskiy, A. B.; Lutsyk, D. S.; Prystansky, R. E. *Chem. Commun.* **1999**, 405.

(14) Lalevée, J.; Allonas, X.; Fouassier, J. P. *J. Org. Chem.* **2007**, *72*, 6434.

(15) Lalevée, J.; Allonas, X.; Jradi, S.; Fouassier, J. P. *Macromolecules* **2006**, *39*, 1872.

(16) Lalevée, J.; Zadoina, L.; Allonas, X.; Fouassier, J. P. *J. Polym. Sci., Part A : Chem.* **2007**, *45*, 2494.

(17) Lalevée, J.; Allonas, X.; Fouassier, J. P. *J. Am. Chem. Soc.* **2002**, *124*, 9613.

(18) Murov, S. L.; Carmichael, I.; Hug, G. L. *Handbook of Photochemistry*; Marcel Dekker: New York, 1993.

(19) Lalevée, J.; Morlet-Savary, F.; Allonas, X.; Fouassier, J.P. *J. Phys. Chem. A* **2006**, *110*, 11605.

(20) Dyachenko, A. G.; Borysenko, M. V.; Pakhovchyshyn, S. V. *Adsorpt. Sci. Technol.* **2004**, *22*, 511.

(21) (a) Chatgilialoglu, C.; Ingold, K. U.; Scaiano, J. C. *J. Am. Chem. Soc.* **1983**, *105*, 3292. (b) Chatgilialoglu, C.; Ingold, K. U.; Scaiano, J. C. *J. Am. Chem. Soc.* **1982**, *104*, 5119. (c) Chatgilialoglu, C.; Rossini, S. *Bull. Soc. Chim. Fr.* **1988**, *2*, 298.

(22) Lalevée, J.; Allonas, X.; Fouassier, J. P. *Chem. Phys. Lett.* **2005**, *415*, 202.

(23) Scaiano, J. C. *J. Phys. Chem.* **1981**, *85*, 2851.

(24) Lalevée, J.; Allonas, X.; Graff, B.; Fouassier, J. P. *J. Phys. Chem. A* **2007**, *111*, 6991.

(25) Rehm, D.; Weller, A. *Isr. J. Chem.* **1970**, *8*, 259.

(26) Alfassi, Z. *Peroxyl Radicals*; Wiley-CH: Chichester, 1997.

(27) Chatgilialoglu, C.; Guarini, A.; Guerrini, A.; Seconi, G. *J. Org. Chem.* **1992**, *57*, 2207.

(28) Lalevée, J.; Allonas, X.; Fouassier, J. P. *Chem. Phys. Lett.* **2007**, *445*, 62.

(29) (a) Chatgilialoglu, C.; Guerrini, A.; Lucarini, M.; Pedulli, G. F.; Carrozza, P.; Da Roit, G.; Borzatta, V.; Luchini, V. *Organometallics* **1998**, *17*, 2169. (b) Zaborovskiy, A. B.; Lutsyk, D. S.; Prystansky, R. E.; Kopylets, V. I.; Timokhin, V. I.; Chatgilialoglu, C. *J. Organomet. Chem.* **2004**, *689*, 2912.

MA702301X